Acta Biochim Biophys Sin 2011, 43: 307–315 | © The Author 2011. Published by ABBS Editorial Office in association with Oxford University Press on behalf of the Institute of Biochemistry and Cell Biology, Shanghai Institutes for Biological Sciences, Chinese Academy of Sciences. DOI: 10.1093/abbs/gmr005.
Advance Access Publication 18 February 2011

Original Article

Depletion of activated hepatic stellate cell correlates with severe liver damage and abnormal liver regeneration in acetaminophen-induced liver injury

Kuntang Shen†, Wenju Chang†, Xiaodong Gao, Hongshan Wang, Weixin Niu, Lujun Song*, and Xinyu Qin*

Department of General Surgery, Institute of General Surgery, Zhongshan Hospital, Shanghai Medical College of Fudan University, Shanghai 200032, China
†These authors contributed equally to this work.
*Correspondence address. Tel: +86-21-64041990-3448 (L.S.)/+86-21-64041990-2663 (X.Q.); Fax: +86-21-64037224 (L.S.)/+86-21-64037224 (X.Q.); E-mail: song.lujun@zs-hospital.sh.cn (L.S.)/qin.xinyu@zs-hospital.sh.cn (X.Q.)

Hepatic stellate cells (HSCs) are important part of the local 'stem cell niche' for hepatic progenitor cells (HPCs) and hepatocytes. However, it is unclear as to whether the products of activated HSCs are required to attenuate hepatocyte injury, enhance liver regeneration, or both. In this study, we performed 'loss of function' studies by depleting activated HSCs with gliotoxin. It was demonstrated that a significantly severe liver damage and declined survival rate were correlated with depletion of activated HSCs. Furthermore, diminishing HSC activation resulted in a 3-fold increase in hepatocyte apoptosis and a 66% decrease in the number of proliferating hepatocytes. This was accompanied by a dramatic decrease in the expression levels of five genes known to be up-regulated during hepatocyte replication. In particular, it was found that depletion of activated HSCs inhibited oval cell reaction that was confirmed by decreased numbers of Pank-positive cells around the portal tracts and lowered gene expression level of cytokeratin 19 (CK19) in gliotoxin-treated liver. These data provide clear evidence that the activated HSCs are involved in both hepatocyte death and proliferation of hepatocytes and HPCs in acetaminophen (APAP)-induced acute liver injury.

Keywords liver regeneration; drug-induced liver injury; hepatic stellate cell; hepatic progenitor cell

Received: October 13, 2010 Accepted: January 18, 2011

Introduction

In normal circumstances, the liver hardly proliferates and is therefore classified as a stable organ. In response to liver injury, mature hepatocytes are able to undergo numerous cycles of cell division to compensate for the cell loss [1]. Serial transplantation experiments have shown that hepatocytes are the functional stem cells of the liver and have almost an infinite capacity to proliferate [2]. However, when proliferative response of mature hepatocytes is overwhelmed or impaired, a reserve cell compartment is activated [3]. This compartment, called the hepatic progenitor cell (HPC) compartment in humans and the oval cell (OVc) compartment in rodents, resides in the smallest and most peripheral branches of the biliary tree, the ductules, and the canals of Hering [4,5]. Acetaminophen (*N*-acetyl-*p*-aminophenol, APAP) is a predictable hepatotoxin that frequently causes acute fulminant hepatic failure in the USA [6]. APAP-induced liver injury causes necrosis of hepatocytes surrounding the central vein caused by a highly reactive metabolite *N*-acetyl-*p*-benzoquinone-imine [7]. With high-dose APAP intoxication, mature hepatocytes may not be able to accomplish full parenchymal reconstitution by mitosis; and thus, regeneration must include activation and hepatocyte differentiation of HPCs. In animal models of liver regeneration and hepatocarcinogenesis, these HPCs are referred to as OVcs [8]. In mice and humans, APAP-induced liver damage is a good and common model for the research of liver injury and regeneration [8,9].

Hepatic stellate cells (HSCs) reside within the perisinusoidal space of Disse in the liver that is lined by parenchymal cells and fenestrated sinusoidal endothelial cells. HSCs display characteristic lipid droplets that contain vitamin A mainly as retinyl palmitate. After liver injury, quiescent HSCs become activated, lose their vitamin A stores, and develop into contractile myofibroblast-like cells, which secrete soluble factors and matrix molecules. It has been widely accepted that HSCs play an important role in the process of embryonic liver development and liver fibrosis [10]. In addition, there is growing evidence that HSCs are also vital to the hepatic regenerative response in adult liver, but further investigation is urgently needed. HSCs are in direct contact with epithelial cells (hepatocytes and HPCs)

and produce growth factors for them [11,12]. Their close anatomic relationship with hepatocytes in the spaces of Disse and around HPCs suggests that they are part of the local 'stem cell niche' for hepatocytes and HPCs [13,14]. However, it is unclear as to whether the products of activated HSCs are required to attenuate hepatocyte injury, enhance hepatocellular regeneration, or both [10]. An important study has identified Foxf1$^{+/-}$ mice after CCl_4 injury exhibits defective HSCs activation associated with severe hepatic apoptosis despite normal cellular proliferation rates [15]. In contrast, following CCl_4 injury, Col-1a1$^{r/r}$ mice showed persistent activation of HSCs and hepatocytes failed to regenerate properly [16]. Overall, the role of HSCs in liver injury and regeneration would be ideally addressed to determine the impact of ablating or inactivating these cells on regeneration of adult liver following injury [10].

In the present study, using APAP plus gliotoxin, we successfully established the model of defective stellate cell activation. Gliotoxin, a fungal metabolite, belongs to the epipolythiodioxopiperazine class of compounds, which was reported to cause apoptosis of activated HSCs by inducing mitochondrial permeability, cytochrome c release, and caspase-3 activation [17,18]. In this study, to demonstrate whether HSC activation directly affected cell death and engraftment in acute liver injury, we established the acute liver injury model that accompanied with sustained activation of HSCs through continuous injections of APAP on mice. Compared with control group based on APAP-induced liver injury, gliotoxin was used to eliminate the activated HSCs in gliotoxin-treated group. We investigated whether depletion of activated HSCs would lead to more serious liver damage and abnormal liver regeneration in the acutely injured liver, specifically by observing the levels of hepatocellular necrosis and apoptosis, and evaluating proliferation capacity of hepatocyte and OVc.

Materials and Methods

Animals

Male C57BL/6J mice (6−8 weeks old) were purchased from Shanghai Laboratory Animal Center, Chinese Academy of Sciences (Shanghai, China). All the animals were maintained in the animal facility of Zhongshan Hospital, Fudan University (Shanghai, China).

Animal models

All animals were fasted overnight before APAP (Sigma-Aldrich, St Louis, USA) treatment. Acute liver injury was induced by APAP dissolved in warmed phosphate-buffered saline (PBS) at the dose of 300 mg/kg with intraperitoneal injection. To assess hepatocyte toxicity following the use of gliotoxin, after one dose of APAP treatment, all animals were randomly divided into two groups: gliotoxin group ($n = 12$) and control group ($n = 12$). Two hours after APAP injection, the gliotoxin group was treated with one dose of gliotoxin (3 mg/kg) dissolved in dimethyl sulfoxide (DMSO) intraperitoneally, control animals received isovolumic DMSO alone as vehicle. Thereafter, blood was collected by retro-orbital puncture and the livers were removed. For establishing the depletion of activated HSCs model, we administered animals three doses of APAP plus gliotoxin (1 mg/kg) by intervals of 3 days each dose, and control animals received APAP plus DMSO alone. We used four animals per group for tissue collections after sacrifice at 24 h after the final APAP treatment and nine animals per group for survival analysis. Blood samples ($n = 4$ per group) were collected at 12, 24, 36, 48, and 96 h after treatment by retro-orbital puncture for analysis of liver enzyme release levels.

Assessment of Kupffer cell activity

Carbon particles were enriched from India ink (Fount India Nr. 17, Pelikan, Germany) by centrifugation (2000 *g*) for 15 min. The supernatant was mixed with five volumes of physiological saline, and 0.1 ml supernatant was injected intrasplenically as previously described [19,20]. To assess the effect of gliotoxin on Kupffer cells, carbon particles were injected 30 min before animals were sacrificed for liver samples.

Assessment of hepatotoxicity

Liver injury was determined by measuring aminotransferase release in the sera and by histologic examination of tissue sections under light microscopy. Serum samples were stored at −80°C until use. Measurement of alanine and aspartate aminotransferase (ALT and AST, respectively) levels was carried out using Thermo Electron (Waltham, USA) infinity ALT and AST reagent (Louisville, USA) according to the manufacturer's instructions.

Bromodeoxyuridine incorporation

Hepatocyte proliferation was estimated by bromodeoxyuridine (BrdU; Sigma-Aldrich) incorporation. Animals were injected intraperitoneally with 0.05 g BrdU/g body weight at 2 h before death. Animals were then killed, and liver samples were obtained, fixed overnight in 4% paraformaldehyde, and processed for histological and immunohistochemical analysis.

Histological and immunohistochemical analysis

For histology, liver tissues were fixed overnight using 4% of paraformaldehyde at 4°C and sections (5 μm) were stained with hematoxylin−eosin (HE; Sigma-Aldrich) to determine morphological changes. HE-stained liver sections were examined and necrosis level was graded using a system

previously described [21]. In brief, sections were dewaxed, hydrated, and washed. After neutralization of endogenous peroxidase and microwave antigen retrieval, slides were pre-incubated with blocking serum and then incubated at 4°C overnight with the primary antibody. Evaluation of murine OVc reactions was performed by Pan-Keratin immunohistochemistry as previously described [8]. Slides were incubated with rabbit polyclonal to wide spectrum cytokeratin (PanK; Abcam, Cambridge, UK) at a dilution of 1:100. After washing with PBS, anti-rabbit peroxidase-labeled antibody (Dako, Carpinteria, USA) was added and incubated for 30 min at room temperature. PanK was visualized by 3,3′-diaminobenzidine chromogen and counterstained with hematoxylin. For fluorescent staining of α-smooth muscle actin (α-SMA) and CD45, sections were incubated with mouse monoclonal anti-α-SMA (Abcam; 1:100) and rat anti-CD45 (eBioscience, San Diego, USA; 1:100), respectively. Labeled cells were visualized with the matched secondary antibody with goat anti-mouse Alexa Fluor 488 (Invitrogen, Carlsbad, USA; 1:500) and goat anti-rat Alexa Fluor 488 (Invitrogen; 1:500) separately. For terminal deoxynucleotidyl transferase-mediated nick-end labeling (TUNEL) staining, we used the fluorescein FragEL DNA fragmentation detection kit (Merck, Darmstadt, Germany) according to the manufacturer's instructions. All sections were examined under Carl-Zeiss microscopy Axiovert 200 (Carl-Zeiss, Jena, Germany) and a computer-assisted image analysis program (AxioVision Ver. 4.0; Carl-Zeiss).

Quantitative real-time polymerase chain reaction

Total RNA was isolated from 50 mg liver tissue using RNAisoTM Plus (TaKaRa, Dalian, China), was reverse transcribed to cDNA using the TwoStep reverse transcription (RT)–polymerase chain reaction (PCR) kit (TaKaRa), and amplified in the ABI 7900HT fast real-time PCR system (Applied Biosystems, Foster City, USA). Cycling parameters were as follows: initial activation at 95°C for 30 s; following 40 cycles for 5 s at 95°C and for 30 s at 60°C. Primers used for amplification were synthesized by TaKaRa as shown in **Table 1**. Specificity of the amplification was checked by melting curve analysis and agarose gel electrophoresis. Gene-specific expression values were normalized to the level of *GAPDH* within each sample. Quantitative RT–PCR data were analyzed using the $2^{-\Delta\Delta Ct}$ method using the SDS 2.1 software according to the manufacturer's instructions (Applied Biosystems).

Table 1 Primers used in this study

Gene	Sequences (5′→3′)
CK19	GGTGCTGGATGAGCTGACTCTG (sense)
	TGGAATCCACCTCCACACTGAC (antisense)
OMS	GCTGGACTCTGACATAGGGTGGA (sense)
	GAGCATCATGCAGCGAGGAC (antisense)
HGF	AGAAATGCAGTCAGCACCATCAAG (sense)
	GATGGCACATCCACGACCAG (antisense)
EGF	CATCATGGTGGTGGCTGTCTG (sense)
	CACTTCCGCTTGGCTCATCA (antisense)
SCF	CTAACTGGTGTGGGCTTAGGAGTGA (sense)
	TGGAGATGGCAGTTGTGCATTTA (antisense)
IL-6	CCACTTCACAAGTCGGAGGCTTA (sense)
	GCAAGTGCATCATCGTTGTTCATAC (antisense)

CK19, cytokeratin 19; *OSM*, oncostatin M; *HGF*, hepatocyte growth factor; *EGF*, epidermal growth factor; *SCF*, stem cell factor; *IL-6*, interleukin 6.

Statistical analysis

Data are presented as the mean ± SD. Statistical significances were determined by two-tailed Student's *t*-tests and, specifically, a log-rank test for survival analysis. The values of $P < 0.05$ were considered significant.

Results

Gliooxin induces defection of activated HSCs

To establish the depletion of activated HSCs model, we used three repeated injections of APAP to cause continuous activation of HSCs; each time after APAP injection, low dose of gliotoxin (1 mg/kg) was applied to abate activated HSCs. The control group used DMSO injections as vehicle after APAP treatment. We measured the number changes of α-SMA-positive HSCs of all animals. In control mice ($n = 4$), 24 h after the final APAP administration, α-SMA fluorescence staining showed marked activation of stellate cells [**Fig. 1(A)**]. However, the number of α-SMA-positive HSCs decreased significantly in gliotoxin-treated mice ($n = 4$) [**Fig. 1(B)**]. A 90% decrease in the number of α-SMA-positive HSCs was observed after gliotoxin treatment (13.1 ± 2.9 compared with 130.1 ± 20.4 in control group; $P < 0.01$) [**Fig. 1(E)**]. The decrease in α-SMA-positive HSCs after gliotoxin resembled the results described by Wright *et al.* [18]. These results demonstrated that gliotoxin treatment may well produce depletion of such continuously activated HSCs. The number of continuously activated HSCs was fewer and there was no significant difference between APAP plus high dose of gliotoxin (3 mg/kg) group and APAP plus vehicle group (data not shown).

Effects of gliotoxin on Kupffer cells and hepatocytes

To evaluate the influence of gliotoxin on Kupffer cells, mice were administered a pulse of carbon to simultaneously demonstrate Kupffer cells toxicity following the use of gliotoxin. It was noteworthy that analysis of carbon particle incorporation in mice treated with APAP plus

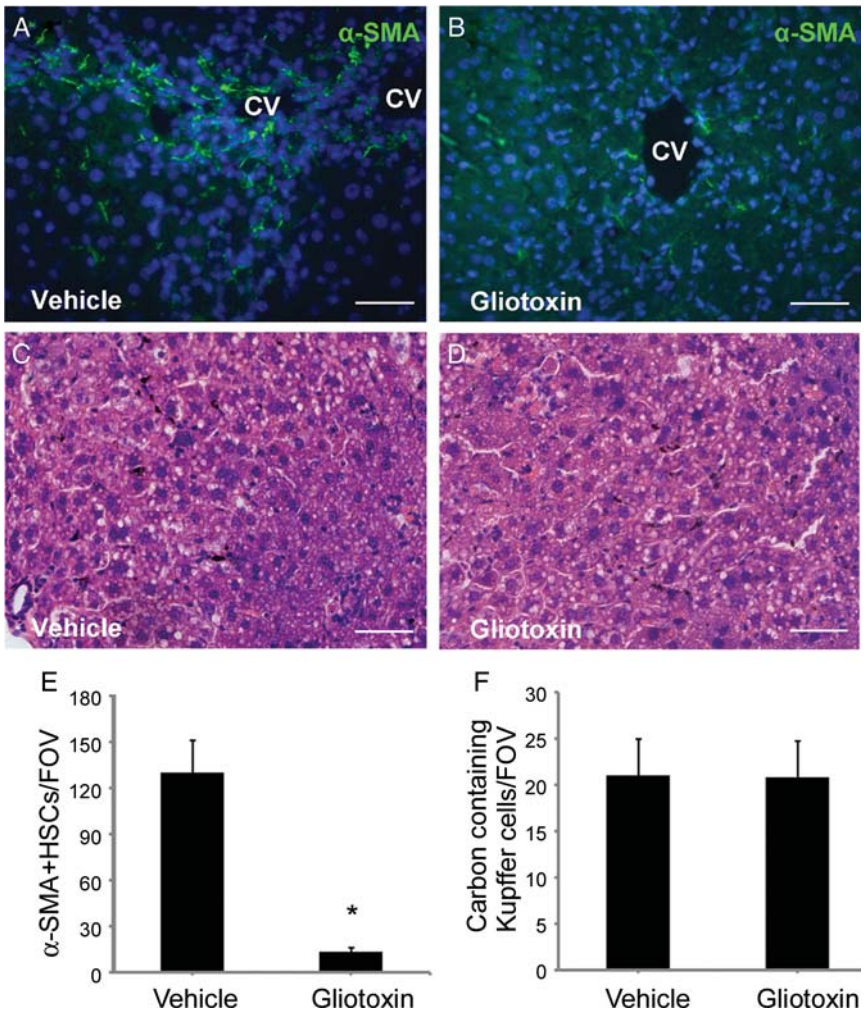

Figure 1 Effects of gliotoxin on HSCs and Kupffer cells To evaluate effects of gliotoxin on HSCs and Kupffer cells, C57BL/6J mice were administered intraperitoneal three doses of APAP (300 mg/kg) with or without gliotoxin (1 mg/kg) injections, with each injection by intervals of 3 days. Mice were sacrificed 24 h after the final APAP treatment. Verification of α-SMA-positive HSCs by immunofluorescence staining of (A) vehicle or (B) gliotoxin treatment was done. Representative 40× images from (C) vehicle-treated and (D) gliotoxin-treated groups show carbon-containing Kupffer cells. (E) Quantification of α-SMA-positive HSCs. (F) Quantification of carbon-containing Kupffer cells. Scale bar=50 μm. Data are expressed as the mean ± standard error of the mean of 10 random high-power fields per animal. *$P < 0.05$. APAP, acetaminophen; α-SMA, α-smooth muscle actin; FOV, field of view; CV; central vein.

DMSO [**Fig. 1(C)**] or APAP plus gliotoxin [**Fig. 1(D)**] showed no differences [**Fig. 1(F)**].

To demonstrate that gliotoxin did not produce concomitant hepatocyte injury, we used APAP plus high dose of gliotoxin (3 mg/kg) or APAP plus vehicle to treat animals, respectively. Histologic tissue sections and serum aminotransferase release were analyzed in both groups. The dose of APAP (300 mg/kg) used in our study for C57BL/6J induced liver injury, indicated by a remarkable increase in serum ALT and AST levels at 12 h, peaking around 24 h with the most serious liver damage, and returning to normal by 4 days [**Fig. 2(B,C)**]. Microscopic evaluation of HE-stained liver sections revealed hepatocytes with similar morphology in both groups at 24 h after APAP treatment (data not shown). Semi-quantitative histological examination of liver tissue confirmed no significant difference [**Fig. 2(A)**]. Moreover, the data of aminotransferase release indicated no significant difference between two groups at the same detection time [**Fig. 2(B,C)**]. Furthermore, cellular proliferation was detected by BrdU incorporation assay. And no significant difference was found between gliotoxin-treated mice and control mice at any detected time points [**Fig. 2(D)**]. These results exclude the effects of gliotoxin on modulating Kupffer cell activity, hepatocyte toxicity, and proliferation, which is consistent with a previous report [19].

Effects of depletion of activated HSCs on liver enzyme release and survival rate

Liver enzyme release levels measured in the peripheral blood provide a good estimate of ongoing liver damage. The peak in liver damage was measured at 24 h after the final APAP treatment, both in control and gliotoxin-treated

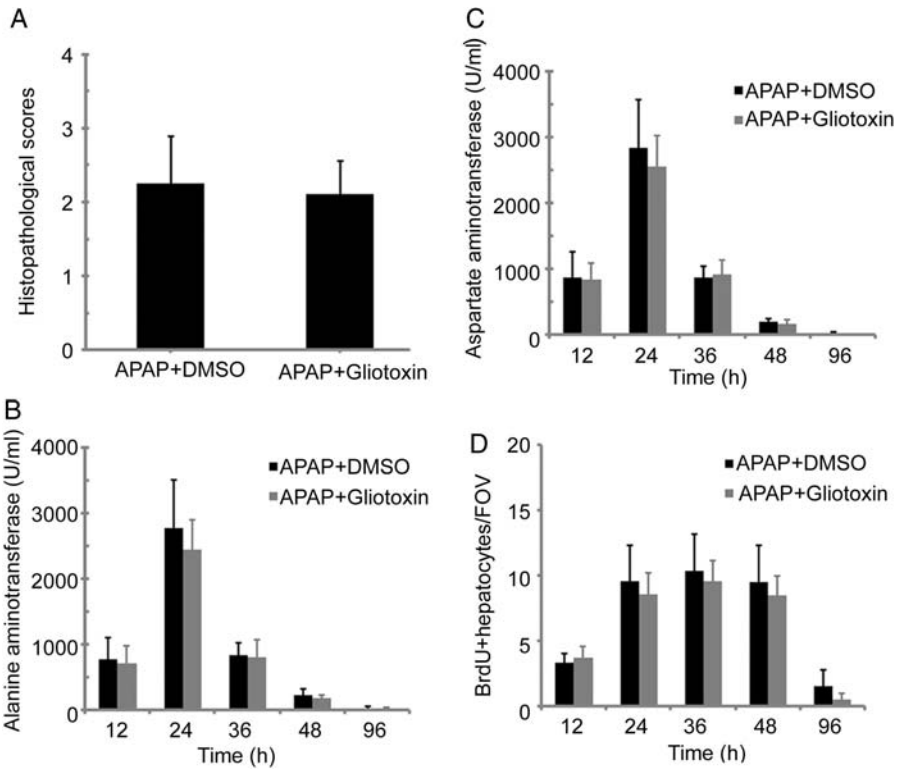

Figure 2 Effects of gliotoxin on hepatocytes To measure the effect of gliotoxin on hepatocytes, mice were injected by one dose of APAP (300 mg/kg) with or without gliotoxin (3 mg/kg). (A) Scores determined by semi-quantitative histological examination. (B) Alanine aminotransferase and (C) aspartate aminotransferase enzyme release levels in peripheral blood samples collected at 12, 24, 36, 48, and 96 h after the final APAP treatment. (D) Quantification of BrdU-positive cells at 12, 24, 36, 48, and 96 h. Data are expressed as the mean ± standard error of the mean of 10 random high-power fields per animal. APAP, acetaminophen; FOV, field of view; BrdU, bromodeoxyuridine.

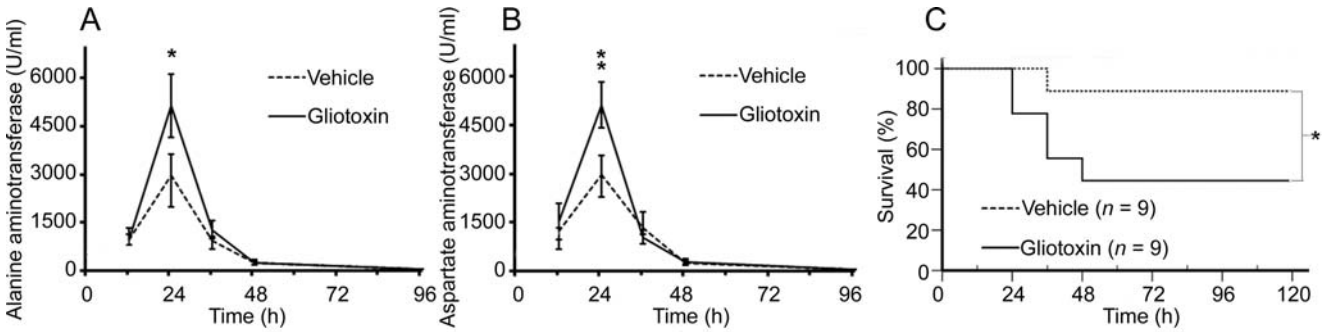

Figure 3 Effects of depletion of activated HSCs on liver enzyme release and survival rate C57BL/6J mice were administered intraperitoneal three dose of APAP (300 mg/kg) with or without gliotoxin (1 mg/kg) injections, with each injection by intervals of 3 days. (A) Alanine aminotransferase and (B) aspartate aminotransferase enzyme release levels in peripheral blood samples collected at 12, 24, 36, 48, and 96 h after the final APAP treatment. (C) Kaplan–Meier survival analysis (log rank test). *$P < 0.05$; **$P < 0.01$. APAP, acetaminophen.

mice. However, the ALT and AST levels were increased by 73% ($P < 0.05$) and 72% ($P < 0.01$), respectively, in gliotoxin-treated mice compared with control mice [**Fig. 3(A,B)**]. For survival analysis, a significant declined survival rate was observed for gliotoxin-treated animals [**Fig. 3(C)**]. Only one animal died during the observation period in control mice, versus 55% in gliotoxin-treated mice ($P < 0.05$). Overall, these results showed that gliotoxin-induced diminished HSCs activation is associated with more severe liver damage and lower survival rate.

Effects of depletion of activated HSCs on hepatocellular necrosis and apoptosis

Microscopic evaluation of HE-stained liver sections revealed hepatocellular death with cytoplasmic vacuolization [**Fig. 4(A,B)**], mononuclear CD45-positive leukocyte infiltration [**Fig. 4(C)**], and distortion of tissue architecture as previously described [22,23] in both groups. However, liver necrosis with immune cell infiltration was more severe in the livers in gliotoxin-treated mice [**Fig. 4(D)**]. Semi-quantitative histological examination of liver tissue confirmed significant

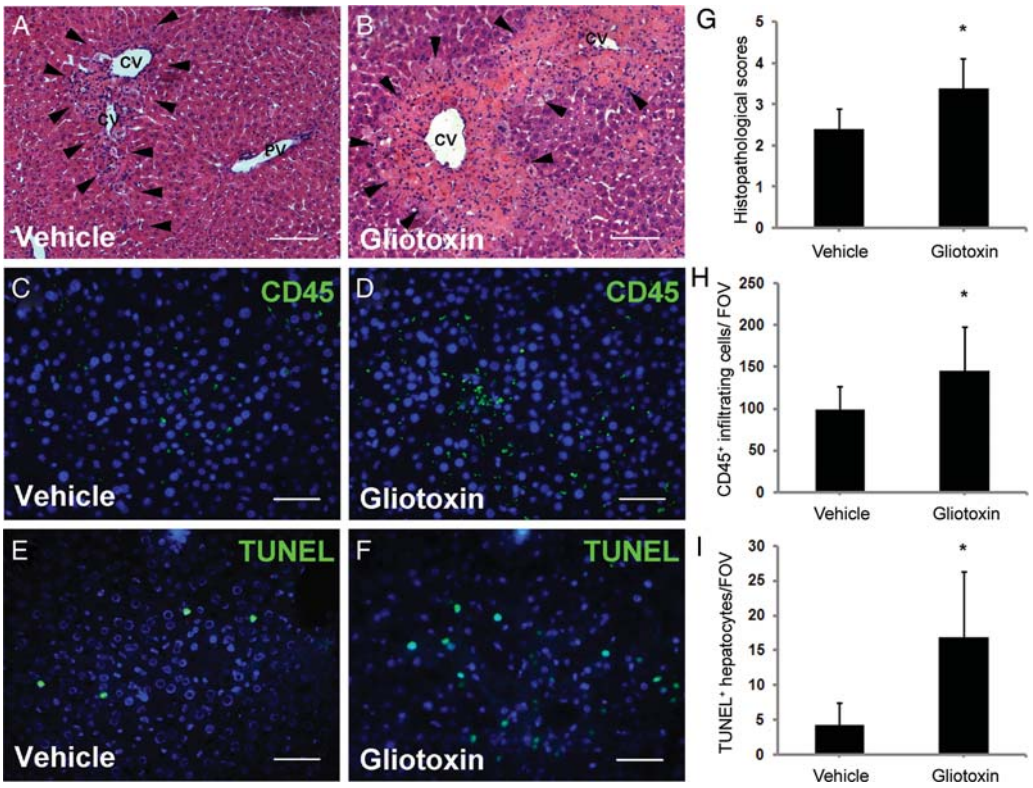

Figure 4 Effect of depletion of activated HSCs on hepatocellular necrosis and apoptosis Mice were sacrificed 24 h after the final APAP treatment. Liver samples were subjected to histological analysis after HE staining. Microscopic high-power field of liver tissue was shown after (A) vehicle or (B) gliotoxin treatment. Necrotic area is indicated by arrowheads. Scale bar = 100 μm. Verification of CD45-positive infiltrates by immunofluorescence staining of (C) vehicle or (D) gliotoxin treatment. Scale bar = 50 μm. Liver sections were stained by TUNEL (green, large for hepatocytes) and counterstained with DAPI (blue). (E) Vehicle-treated and (F) gliotoxin-treated were shown. Scale bar = 50 μm. (G) Scores determined by semi-quantitative histological examination. (H) Quantification of infiltrating immune cells. (I) Quantification of TUNEL-positive hepatocyte nuclei by digital image analysis. Data are shown as thee mean ± standard error of the mean of 10 random high-power fields per animal. *$P < 0.05$. CV, central vein; PV, portal vein; HE, hemotoxylin–eosin; TUNEL, terminal deoxynucleotidyl transferase-mediated nick-end labeling; DAPI 4,6-diamino-2-phenyl indole; FOV, field of view.

differences between the two groups [**Fig. 4(G)**]. The average score in gliotoxin-treated group was 2.4 ± 0.5 and 3.4 ± 0.7 for vehicle-treated animals ($P < 0.01$). A 47% increase in the number of infiltrating CD45-positive immune cells was observed after gliotoxin treatment (146.5 ± 52.9 per field of view in treatment group versus 99.1 ± 26.4 per field of view in control group; $P < 0.01$) [**Fig. 4(H)**]. Likewise, gliotoxin-treated mice showed increased pericentral apoptosis [**Fig. 4(F)**] using TUNEL assay, while few apoptotic cells were found in vehicle-treated hepatocytes [**Fig. 4(E)**]. Quantification revealed a 3-fold increase in TUNEL-positive hepatocyte nuclei (16.9 ± 9.3 per field of view) when compared with control mice (4.3 ± 3.0 per field of view; $P < 0.05$) [**Fig. 4(I)**]. These results demonstrated that depletion of activated HSCs correlates with more severe hepatocellular necrosis and apoptosis.

Depletion of activated HSCs is accompanied by abnormal hepatocytes replication

Inhibition of endogenous mature hepatocytes mitosis program represents another potential mechanism of the declined survival rate after liver injury. To determine the effect of abating activated HSCs on replication of mature hepatocytes, BrdU-positive hepatocytes were quantified and compared with vehicle-treated mice. Qualitatively, few BrdU-positive hepatocytes were seen in gliotoxin-treated livers [**Fig. 5(B)**], while many BrdU-positive hepatocytes were observed in control mice [**Fig. 5(A)**]. A 66% decrease in the number of proliferating liver cells (3.8 ± 1.9 per field of view versus 11.3 ± 5.2 per field of view in control group; $P < 0.01$) [**Fig. 5(E)**]. Evaluation of expression levels of five genes [oncostatin M (*OSM*), hepatocyte growth factor (*HGF*), epidermal growth factor (*EGF*), stem cell factor (*SCF*), and interleukin 6 (*IL-6*)] known to be up-regulated during liver regeneration revealed visibly lower expression levels in gliotoxin-treated livers by fluorescent quantitative RT–PCR [**Fig. 5(G)**]. Quantitative analysis demonstrated that expression levels of all five genes were significantly declined after gliotoxin treatment. Decreases ranged from 0.2 to 4.3 folds compared with the control group [**Fig. 5(G)**]. These results demonstrate that abating activated HSCs inhibit the capacity of mature hepatocytes replication.

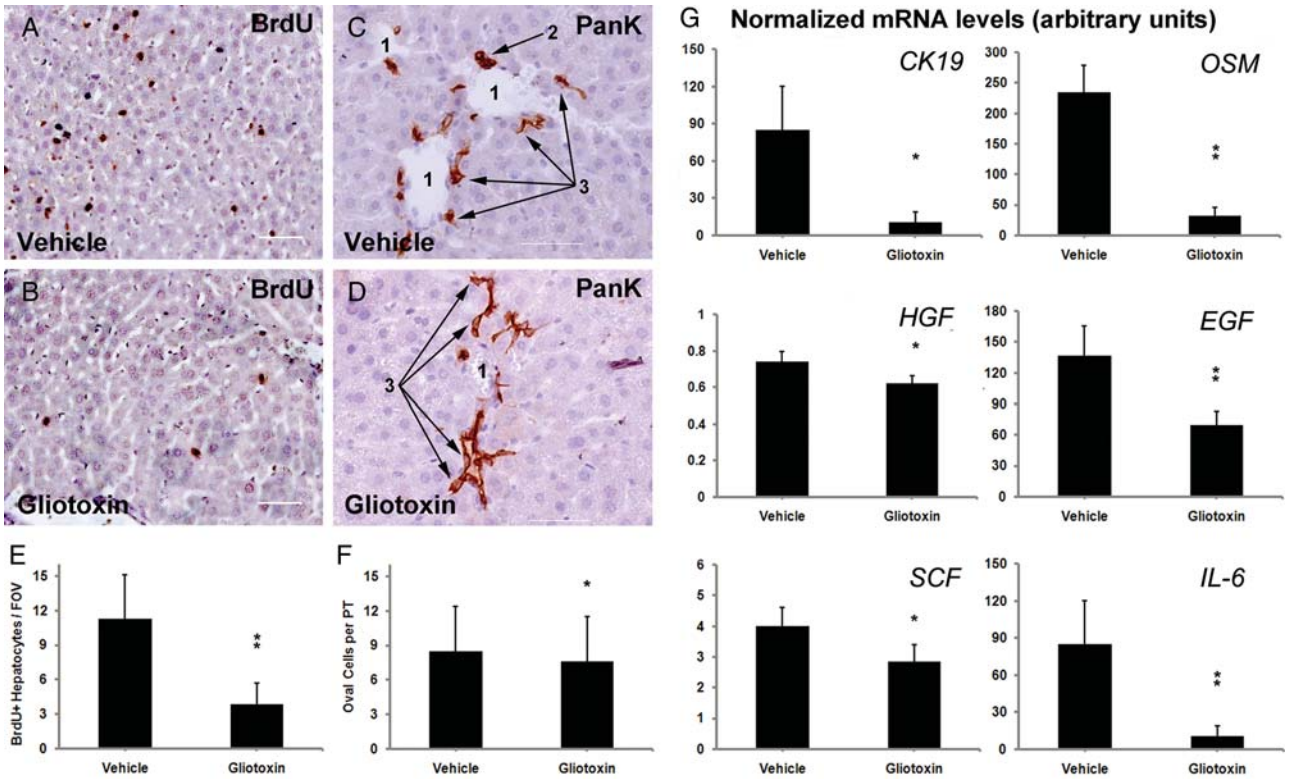

Figure 5 Effect of depletion of activated HSCs on hepatocytes replication and OVc reaction Liver samples were analyzed 24 h after the final APAP treatment. Sections were stained for BrdU (dark brown nuclei, large for hepatocytes). Representative 40× image from (A) control and (B) gliotoxin-treated mice. Sections were stained for PanK (dark brown). (C,D) Representative 40× image shows that heterogeneous population of expanding PanK-positive cells varying in size and morphology with mostly oval nuclei. 1, portal vein; 2, bile duct; and 3, OVcs. (E) Quantification of BrdU-positive hepatocytes. (F) Quantification of PanK-positive cells. Data are expressed as the mean ± standard error of the mean for 10 random fields per animal. (G) Quantification of changes in gene expression by fluorescent RT–PCR. Scale bar = 50 μm. $*P < 0.05$; $**P < 0.01$. BrdU, bromodeoxyuridine; FOV, field of view; PanK, biliary cytokeratins; PT, portal tract; *CK19*, cytokeratin; *OSM*, oncostatin M; *HGF*, hepatocyte growth factor; *EGF*, epidermal growth factor; *SCF*, stem cell factor; *IL-6*, interleukin 6.

Contribution of the depletion of activated HSCs to OVc reaction

In addition to mature hepatocytes replicative capacity, we also evaluated OVc reaction in APAP-induced liver injury with or without gliotoxin treatment. OVc express phenotypical markers of both the biliary epithelium (cytokeratins CK7 and CK19), and the hepatocyte lineages (α-fetoprotein and albumin). We used anti-PanK antibodies to detect OVc that appeared singly or in irregular strings without lumens in the small portal tracts as previously described [4,8]. OVc defined as densely cytokeratin-positive cells with oval/cuboidal morphology and high nuclear-to-cytoplasmic ratio and could be easily classified from small bile duct with lumens [**Fig. 5(C,D)**]. Quantification of OVc around the portal tracts with portal veins of cross-sectional areas $<3000\ \mu m^2$ showed a statistically significant decrease ($P < 0.05$) in OVc after gliotoxin treatment compared with control mice [**Fig. 5(C,D)**]. For gliotoxin-treated mice ($n = 245$; the number of counted portal tracts), the average number of OVc per portal tract was 7.6 ± 4.0 and 8.5 ± 4.0 for the control group ($n = 225$) [**Fig. 5(F)**]. Moreover, we evaluated the gene expression levels of *CK19* that up-regulated during OVc reaction. Quantitative analysis demonstrated that the expression level of *CK19* was significantly declined ($P < 0.05$) after gliotoxin treatment compared with the control mice [**Fig. 5(G)**]. This result is consistent with immunohistochemical staining of anti-PanK and indicates that OVc reaction declines with depletion of activated HSCs.

Discussion

Liver regeneration driven by epithelial cell (hepatocyte and HPC) proliferation is necessary for tissue repair and survival after acute liver injury [24]. The induction of epithelial cell proliferation depends on cross-talk between epithelial cells and nonparenchymal liver cells, such as HSCs [11]. In response to injury, HSCs differentiate to myofibroblasts, and secrete extracellular matrix and growth factors that are involved in liver regeneration [14]. Although this view is widely accepted, however, it is unclear whether products of activated stellate cells are required to attenuate hepatocyte

injury, enhance epithelial cell regeneration, or both [10]. In this study, we performed 'loss of function' studies by depleting activated HSCs with gliotoxin. The data showed that the number of continuously activated HSCs was fewer and has no significant difference between the groups of APAP plus high dose of gliotoxin (3 mg/kg) and APAP plus vehicle. However, we observed a large number of activated HSCs after three repeated injections of APAP, and there was a significant difference between the gliotoxin group and control group. This is because that sustained activation of HSCs requires repeated liver damages as the prerequisite, and gliotoxin would only cause apoptosis of activated HSCs rather than quiescent ones [17,18]. Based on the 'loss of function' studies, we showed that a significantly declined survival rate and a deterioration of liver enzyme release correlate with the depletion of activated HSCs. Increased liver damage and inhibition of hepatocyte replication is associated with diminished HSCs activation after gliotoxin treatment. In addition, we provided the clear evidence that defective stellate cell activation causes a significant reduction in OVc reaction after APAP-induced acute liver injury.

Previous study showed that α-SMA was a good marker for activated stellate cells [18]. We exhibited defective HSCs activation as evidenced by decreased α-SMA-positive HSCs with immunohistochemical staining. Moreover, when gliotoxin treatment produced depletion of such activated HSCs, we also evaluated effects of gliotoxin on Kupffer cells and hepatocytes. Previous studies indicated that Kupffer cells had an important protective function in the acute liver injury and could stimulate liver regeneration [25,26]. In this study, Kupffer cell activity was not affected by gliotoxin, which was consistent with a previous report [19]. Moreover, analysis of histologic tissue sections, serum aminotransferase release, and BrdU-positive hepatocytes demonstrated that gliotoxin had no significant effects on hepatocyte toxicity and proliferation. Taken together, these results rule out the effects of gliotoxin itself on liver injury and regeneration [19,20].

We detected that diminished stellate cell activation was associated with both the increased hepatocellular necrosis and apoptosis in gliotoxin-treated livers and the decreased gene expression levels of *HGF* and *IL-6*, and other soluble factors (*EGF*, *SCF*, and *OSM*) implicated in the protection of hepatocytes against death after liver injury [12]. Interestingly, the activated HSCs are a major source of HGF and IL-6 [14], suggesting that depletion of activated HSCs in gliotoxin-treated livers may contribute to severe hepatocellular necrosis and apoptosis. Furthermore, increased CD45-positive cells were observed with the depletion of activated HSCs. Because the liver innate immune system plays a major role in determining the progression and severity of APAP-induced hepatotoxicity [21,22], elevated CD45-positive cells reflect accumulated neutrophils and lymphocytes in the liver that contributes to severe liver injury. Previous study indicated that activated HSCs could play an important role in immune modulatory activity both *in vivo* and *in vitro* [27,28]. It has previously been shown that gliotoxin was an immunosuppressive secondary metabolite and weakens inflammatory response [29]. Our data showed that gliotoxin-induced depletion of activated HSCs was associated with more severe inflammatory response. The relative effects and mechanisms need to be confirmed and elaborated, respectively, further. We speculate that compared with decrease inflammatory response of gliotoxin, the depletion of activated HSCs may lead to more exacerbated immune cell infiltration and enhanced inflammatory response.

When it comes to the role of diminished HSCs activation in hepatocyte proliferation, there are still some controversies. In response to CCl_4 injury, $Foxf1^{+/-}$ mice exhibited defective HSC activation, as assessed by α-SMA expression, which was associated with increased hepatocyte apoptosis but normal hepatocyte proliferation [15]. However, in a similar approach, in $p75NTR^{-/-}$ mice, HSCs failed to differentiate to myofibroblasts and inhibited hepatocyte proliferation after liver injury [30]. In this study, we found a 66% decrease in the number of proliferating hepatocytes, which was associated with diminished stellate cell activation. In addition, we detected decreased gene expression, ranging from 0.2 to 4.3 folds, of five genes known to be up-regulated during hepatocyte replication [12]. An important finding in this study was that depletion of activated HSCs inhibited OVc reaction that was confirmed by decreased numbers of PanK-positive cell around the portal tracts [4] and declined gene expression levels of *CK19* in gliotoxin-treated livers. We applied Pan-CK immunohistochemical staining, and *CK19* gene expression level to evaluate OVc reaction. Although *CK19* gene expresses in both bile duct and OVc, the APAP-induced liver injury that only leads to hepatocytes damage would not cause bile duct injury. Therefore, the gene expression level of *CK19* would well evaluate the proliferation of OVc. Our results conclude that HSC activation is necessary for the proliferation of both hepatocytes and OVc in APAP-induced liver injury, although it is difficult to tease out the potential mechanisms based on these data alone. In the future, much better models of eliminated activated HSCs need to be established to further confirm these effects and elaborate relative mechanisms.

In conclusion, the current study showed that activated HSCs were involved in both hepatocyte dead and epithelia cell proliferation in APAP-induced acute liver injury. As part of the local 'stem cell niche' for hepatocytes and HPCs, elucidation of the role and mechanism of HSCs may shed new light on liver injury therapy.

Funding

This work was supported by a grant from Shanghai Municipal Government (No. 04DZ19505).

References

1 Ankoma-Sey V. Hepatic regeneration-revisiting the myth of prometheus. News Physiol Sci 1999, 14: 149–155.
2 Overturf K, Al-Dhalimy M, Finegold M and Grompe M. The repopulation potential of hepatocyte populations differing in size and prior mitotic expansion. Am J Pathol 1999, 155: 2135–2143.
3 Dabeva MD and Shafritz DA. Hepatic stem cells and liver repopulation. Semin Liver Dis 2003, 23: 349–362.
4 Kuwahara R, Kofman AV, Landis CS, Swenson ES, Barendswaard E and Theise ND. The hepatic stem cell niche: identification by label-retaining cell assay. Hepatology 2008, 47: 1994–2002.
5 Zhang L, Theise N, Chua M and Reid LM. The stem cell niche of human livers: symmetry between development and regeneration. Hepatology 2008, 48: 1598–1607.
6 Chun LJ, Tong MJ, Busuttil RW and Hiatt JR. Acetaminophen hepatotoxicity and acute liver failure. J Clin Gastroenterol 2009, 43: 342–349.
7 Ito Y, Bethea NW, Abril ER and McCuskey RS. Early hepatic microvascular injury in response to acetaminophen toxicity. Microcirculation 2003, 10: 391–400.
8 Kofman AV, Morgan G, Kirschenbaum A, Osbeck J, Hussain M, Swenson S and Theise ND. Dose- and time-dependent oval cell reaction in acetaminophen-induced murine liver injury. Hepatology 2005, 41: 1252–1261.
9 Theise ND, Saxena R, Portmann BC, Thung SN, Yee H, Chiriboga L and Kumar A, *et al*. The canals of Hering and hepatic stem cells in humans. Hepatology 1999, 30: 1425–1433.
10 Friedman SL. Hepatic stellate cells: protean, multifunctional, and enigmatic cells of the liver. Physiol Rev 2008, 88: 125–172.
11 Mabuchi A, Mullaney I, Sheard PW, Hessian PA, Mallard BL, Tawadrous MN and Zimmermann A, *et al*. Role of hepatic stellate cell/hepatocyte interaction and activation of hepatic stellate cells in the early phase of liver regeneration in the rat. J Hepatol 2004, 40: 910–916.
12 Taub R. Liver regeneration: from myth to mechanism. Nat Rev Mol Cell Biol 2004, 5: 836–847.
13 Yin L, Lynch D and Sell S. Participation of different cell types in the restitutive response of the rat liver to periportal injury induced by allyl alcohol. J Hepatol 1999, 31: 497–507.
14 Roskams T. Relationships among stellate cell activation, progenitor cells, and hepatic regeneration. Clin Liver Dis 2008, 12: 853–860.
15 Kalinichenko VV, Bhattacharyya D, Zhou Y, Gusarova GA, Kim W, Shin B and Costa RH. Foxf1$^{+/-}$ mice exhibit defective stellate cell activation and abnormal liver regeneration following CCl4 injury. Hepatology 2003, 37: 107–117.
16 Issa R, Zhou X, Trim N, Millward-Sadler H, Krane S, Benyon C and Iredale J. Mutation in collagen-1 that confers resistance to the action of collagenase results in failure of recovery from CCl_4-induced liver fibrosis, persistence of activated hepatic stellate cells, and diminished hepatocyte regeneration. FASEB J 2003, 17: 47–49.
17 Kweon YO, Paik YH, Schnabl B, Qian T, Lemasters JJ and Brenner DA. Gliotoxin-mediated apoptosis of activated human hepatic stellate cells. J Hepatol 2003, 39: 38–46.
18 Wright MC, Issa R, Smart DE, Trim N, Murray GI, Primrose JN and Arthur MJ, *et al*. Gliotoxin stimulates the apoptosis of human and rat hepatic stellate cells and enhances the resolution of liver fibrosis in rats. Gastroenterology 2001, 121: 685–698.
19 Benten D, Kumaran V, Joseph B, Schattenberg J, Popov Y, Schuppan D and Gupta S. Hepatocyte transplantation activates hepatic stellate cells with beneficial modulation of cell engraftment in the rat. Hepatology 2005, 42: 1072–1081.
20 Joseph B, Malhi H, Bhargava KK, Palestro CJ, McCuskey RS and Gupta S. Kupffer cells participate in early clearance of syngeneic hepatocytes transplanted in the rat liver. Gastroenterology 2002, 123: 1677–1685.
21 Liu ZX, Han D, Gunawan B and Kaplowitz N. Neutrophil depletion protects against murine acetaminophen hepatotoxicity. Hepatology 2006, 43: 1220–1230.
22 Liu ZX, Govindarajan S and Kaplowitz N. Innate immune system plays a critical role in determining the progression and severity of acetaminophen hepatotoxicity. Gastroenterology 2004, 127: 1760–1774.
23 Parekkadan B, van Poll D, Suganuma K, Carter EA, Berthiaume F, Tilles AW and Yarmush ML. Mesenchymal stem cell-derived molecules reverse fulminant hepatic failure. PLoS One 2007, 2: e941.
24 Duncan AW, Dorrell C and Grompe M. Stem cells and liver regeneration. Gastroenterology 2009, 137: 466–481.
25 Ju C, Reilly TP, Bourdi M, Radonovich MF, Brady JN, George JW and Pohl LR. Protective role of Kupffer cells in acetaminophen-induced hepatic injury in mice. Chem Res Toxicol 2002, 15: 1504–1513.
26 Meijer C, Wiezer MJ, Diehl AM, Schouten HJ, Meijer S, van Rooijen N and van Lambalgen AA, *et al*. Kupffer cell depletion by CI2MDP-liposomes alters hepatic cytokine expression and delays liver regeneration after partial hepatectomy. Liver 2000, 20: 66–77.
27 Chen CH, Kuo LM, Chang Y, Wu W, Goldbach C, Ross MA and Stolz DB, *et al*. *In vivo* immune modulatory activity of hepatic stellate cells in mice. Hepatology 2006, 44: 1171–1181.
28 Yu MC, Chen CH, Liang X, Wang L, Gandhi CR, Fung JJ and Lu L, *et al*. Inhibition of T-cell responses by hepatic stellate cells via B7-H1-mediated T-cell apoptosis in mice. Hepatology 2004, 40: 1312–1321.
29 Kupfahl C, Geginat G and Hof H. Gliotoxin-mediated suppression of innate and adaptive immune functions directed against Listeria monocytogenes. Med Mycol 2006, 44: 591–599.
30 Passino MA, Adams RA, Sikorski SL and Akassoglou K. Regulation of hepatic stellate cell differentiation by the neurotrophin receptor p75NTR. Science 2007, 315: 1853–1856.